Numerical Simulation of Si Nanosecond Laser Annealing by COMSOL Multiphysics

M. Darif*, N. Semmar
GREMI-UMR6606, CNRS-Université d'Orléans, 14 rue d'Issoudun, BP 6744, F-45067 Orléans Cedex, France
*Corresponding author: mohamed.darif@univ-orleans.fr

Abstract: 2D transient heat conduction model was created in COMSOL Multiphysics as a simulation of temperature change in material irradiated by KrF beam (248 nm, 27 ns) confined on the silicon's surface (10 - 50 nm).

In this paper, the obtained results are shown and discussed in case of bulk Silicon. The heat source is distributed in time with 'gate' and 'gaussian' shapes. The thermal properties values obtained, in case of 'gate' shape, were compared with those obtained in case of 'gaussian' shape. The returned result concerns surface temperature versus time and laser fluence (800-1300 mJ/cm²). Typically, over a laser fluence of 2000 mJ/cm², ablation process occurs on Silicon surface.

Keywords: COMSOL Multiphysics simulation, Laser heating, Silicon thermal properties.

1. Introduction

The importance of laser thermal processing (LTP) and thermal properties investigation of bulk and complex materials is still increasing. Lasers are used in material processing (cutting, drilling, welding, marking etc.), pulsed lasers are often used to heat, to melt or to ablate the surface part exact amount of energy and the inner part stays without changes.

Excimer laser crystallization is an efficient technology for obtaining high-performance poly-Si TFTs [**7**] for advanced flat panel display applications. In order to improve both the device performance and uniformity, high-quality poly-Si films with controlled grain size and location are required.

The aim of this work is to control the melting thickness (20-50 nm) by pulsed laser treatment, in order to recrystallized a surface layer which amorphized by ionic implantation and to reactivate the doping agents of this one. For this, simulation by COMSOL Multiphysics is used to predict the melting kinetics by pulsed lasers. To accomplish this objective, several methods [**1-5**] have been developed utilizing spatially selective melting and lateral temperature modulation. A melt-mediated transformation scenario has been proposed [**6-8**] suggesting that the recrystallized Si morphology is determined by complex phase transformations. However, the evolution of these melting and resolidification phenomena [**3**] has not been experimentally verified by direct temperature measurements.

One of demo examples in COMSOL Multiphysics solves interaction of laser with Silicon sample but with considering negligible width of laser beam. In this example silicon is assumed to be semitransparent and Lambert-Beer law is used for the energy (photons) absorption in depth.

A model of laser interaction with moving material in COMSOL was created by Bianco et al. [**9**]. They simulated moving laser with gaussian distribution, infinite or semi-infinite 3D sample brick-typa worke-piece, radiative and convective heat loses.

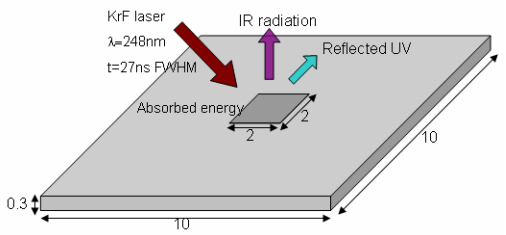

Figure 1: Schematic view of laser beam interaction with material surface (dimensions in mm)

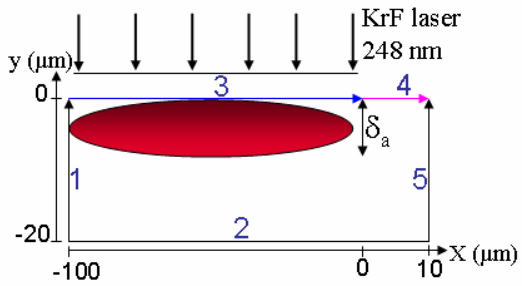

Figure 2. Sketch of selected part of bulk sample for modeling in COMSOL with numbers of boundary conditions.

In the present paper one example of laser heating a sample with dimensions 10*10*0.3 mm^3 is solved with affected area 2*2 mm^2 (Figure 1). The time resolution is in order of ns due to the pulse duration of the KrF laser which is closely 27 ns (FWHM) (Full

Width at Half Maximum). The Numerical procedure is developed under COMSOL project and treated with 1.0 nm mesh size in the photon absorbing area (boundary 3) (Figure 2). In the *subdomain* zone the mesh size is close to 100 nm.

The returned result concerns surface temperature versus time and laser fluence (energy density), and also temperature versus depth (y).

2. Governing equations

The heat source is distributed in time with 'gate' and 'gaussian' shapes (Figure 3). The returned results were almost simulated by conduction/diffusion models (B. Dragnea et al., PRL 1999) that are not well appropriate to the understanding of transport phenomena in the case of silicon.

Mathematical formulation of problem is described by volume equation of heat conduction

$$\rho C_p \frac{\partial T}{\partial t} - \nabla\left(k \nabla T\right) = Gt \qquad (1)$$

Where ρ is material density, C_p specific heat capacity, T temperature, t time and k thermal conductivity. Gt is the heat source distribution in depth (Y) according to the Beer-lambert law (Figure 4); it's described by following equation :

$$Gt\left(y,t\right) = I\left(t\right).\left(1 - R\left(T\right)\right).\frac{e^{\frac{-y}{\delta a}}}{\delta a} \qquad (2)$$

With:

$I\left(t\right)$ [W/cm²]: Time distribution of the laser beam intensity.

The sample can be simplified to 2D rectangle, x coordinate for width and y coordinate for depth (Figure 2). Only interface between heated and unheated part is solved i.e. a half of the sample is irradiated by laser and another half is not irradiated. As a source of heat it is used the energy absorbed in volume.

The specular reflectivity at $\lambda = 248\,nm$ at 300 K on monocrystalline silicon is 61%. Melted silicon has the properties of a metal, i.e. high reflectivity, in general 73% [**4**]. The penetration depth δ_a under these last conditions is $\delta_a \approx 6\,nm$ [**2**], it depends on optical properties of semi-conductor (Si); refractive index n_1 and extinction coefficient n_2.

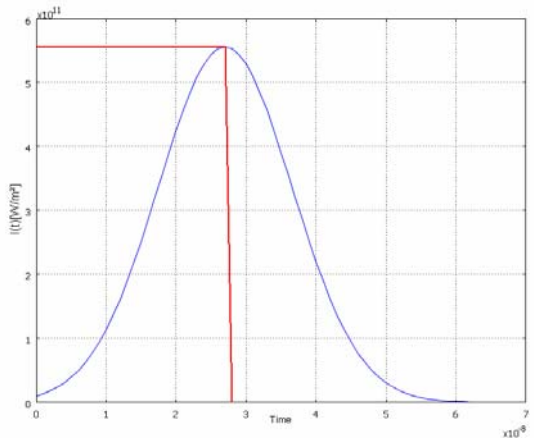

Figure 3: Time distribution of the incident heat flux density : Gate shape and Gaussian shape

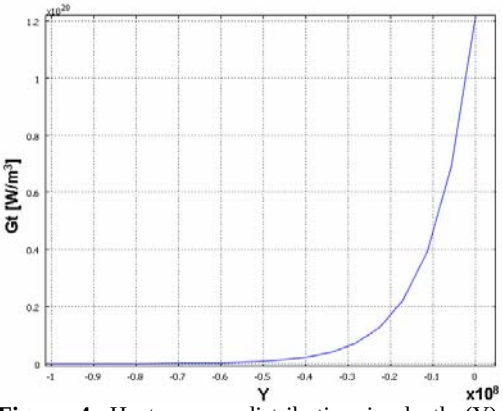

Figure 4: Heat source distribution in depth (Y): Beer-lambert law

$$n = n_1 + i n_2 \qquad (3)$$

Absorption coefficient α can be expressed by:

$$\alpha = \frac{2\omega n_2}{c} = \frac{4\pi n_2}{\lambda} = \frac{1}{\delta a} \qquad (4)$$

Where ω is the circular frequency and c speed of light. α is used in Beer-lambert law as following

$$I\left(y\right) = I_0 . e^{-\alpha |y|} \qquad (5)$$

Where $I\left(y\right)$ is the depth dependent laser intensity, I_0 is the intensity of the surface and $|y|$ is the depth as indicated in relationship (2).

Surface boundary condition for irradiated area (boundary 3 in figure 2) is described by equation (6)

$$\vec{n}.\left(k \nabla T\right) = q_0 + h\left(T_{\inf} - T\right) + \sigma.\varepsilon\left(T_{amb}^4 - T^4\right) \qquad (6)$$

Where $\vec{n}$ is the normal vector, q_0 the surface heat flux, h the convective heat transfer coefficient, T_{inf} external temperature, σ Stefan-Boltzmann constant, ε emissivity and T_{amb} ambient temperature.

The unheated area (boundary 4) has the equation of the same shape as boundary 3 only without the heat source distribution term Gt. Left bottom and right side (boundaries 1,2 and 5) are thermally insulated (adiabatic conditions), that means:

$$\vec{n}.(k\nabla T) = 0 \qquad (7)$$

3. COMSOL realization

For the thermal model, *Heat transfer mode* and *Transient analysis* in *Conduction* type of heat transfer, have been chosen in order to solve the heat conduction equation. Sample geometry is made of a rectangle with dimensions in Figure 2.

In *global expressions* there are created variables and *constants* necessary for modeling laser pulse [Table 1] i.e. absorbed energy, affected area, shape of pulse (absorbed heat flux distribution in time) and material emissivity. The initial temperature of the *subdomain* is set to 293 K.

For the heat source, energy is absorbed in volume. Surface boundary condition includes thermal radiation and heat transfer to ambient room. Other boundary conditions were considered as thermal insulation (adiabatic conditions). Mesh elements in *subdomain* has maximal size 100 nm. On the surface (boundary 3) the finer element distribution with maximal size 2 nm is used

In *solver parameters* time ranges from 0 to 60 ns with a step of 2 ns. For solving default solver is used.

In *Postprocessing* mode there is selected "Cross-Section Plot parameters/Point" and inserted coordinates [-0.8e-4 ; 0] for surface temperature visualization.

4. Simulation results in case of crystalline-Si

The returned result concerns surface temperature versus time and laser fluence (Figure 5), temperature profile in depth (y) (Figure 6) for the gate shape and gaussian shape time distribution.

The melting kinetics (Melted thickness and liquid/solid interface velocity) is also computed and will be compared to the experimental results (TEM and MEB Techniques) in future work.

Notice that for laser fluence lower than 1050 mJ/cm² (i.e. threshold of melting in case of gate shape), the execution time is close to few minutes. However, for higher laser fluence, when the melting process starts, the execution time increases dramatically to many hours.

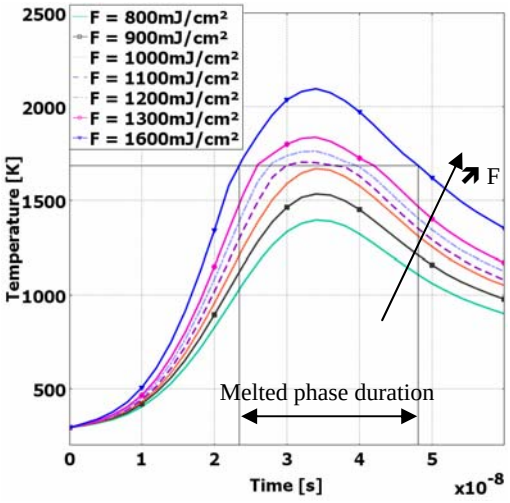

a)

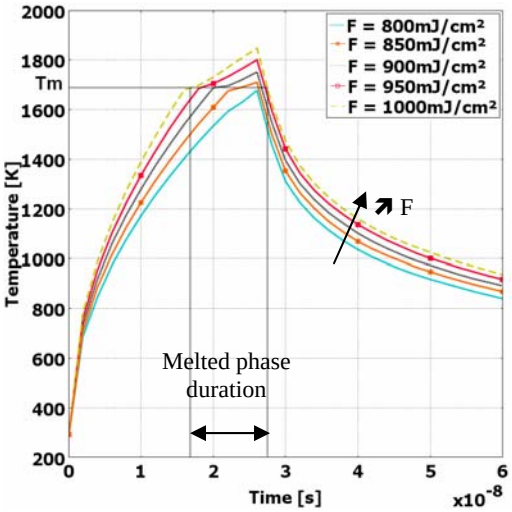

b)

Figure 5 : Point [-0.8e-4 ; 0] temperature versus time at different laser fluences (F). a) for Gaussian shape, b) for Gate shape

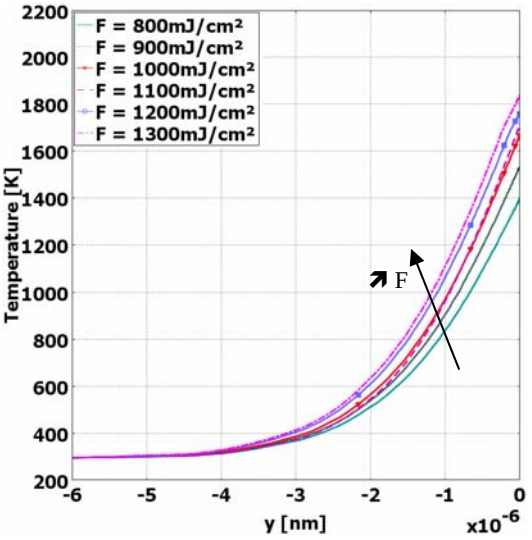

a)

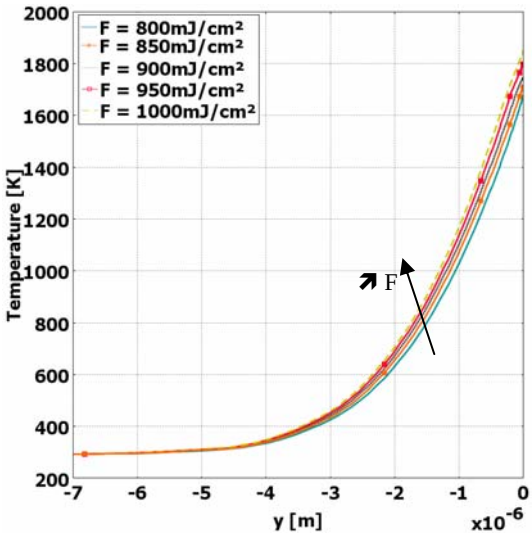

b)

Figure 6: Temperature profile versus depth (Y) at time t = t_{max}. a) for Gaussian shape, b) for Gate shape

As increasing depth position (Y), the maximal temperature decreases dramatically to room temperature at 6 µm as can be seen from Figure 6. Figure 7 introduces temperature field evolution for absorbed laser fluence F = 1000 mJ/cm² in the case of gate shape time distribution.

As reported in figures 5 and 8, in the case of gate shape time distribution, the melting phase starts for laser fluence F = 850 mJ/cm² However, the threshold of melting occurs in the case of Gaussian shape, for laser fluence higher than the last one (F = 1050 mJ/cm²). One should notice that for similar laser fluence higher than the lowest melting threshold (1050 mJ/cm² in case of gaussian shape) the melted layer and phase duration are higher in the case of the gate shape (Figure 9 and Figure 5).

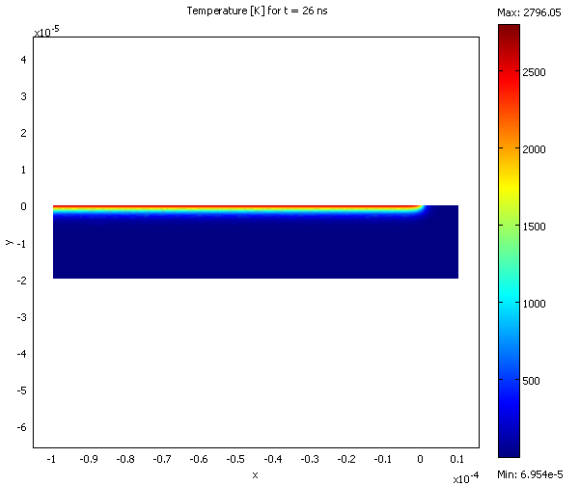

a) t = 26 ns

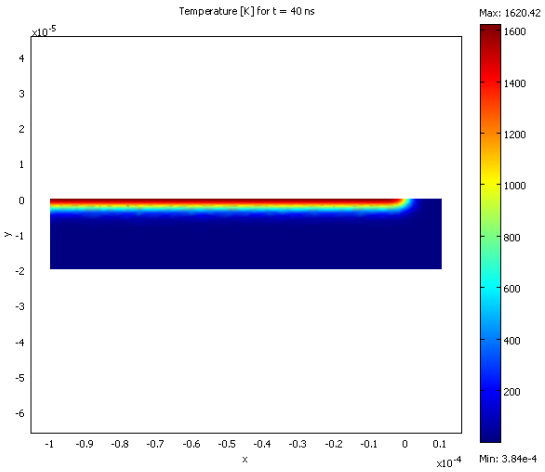

b) t = 40 ns

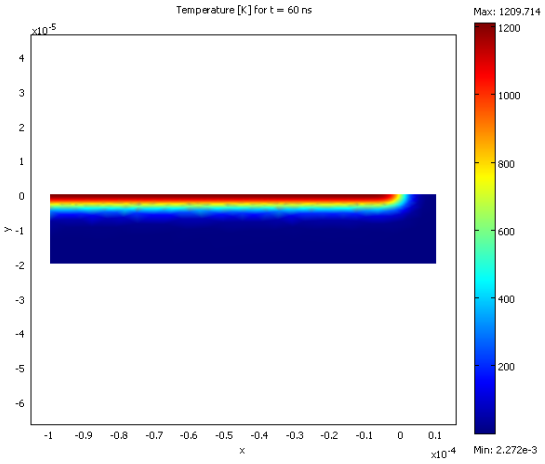

c) t = 60 ns

Figure 7: Temperature field evolution for time a) t = 26 ns, b) t = 40 ns, c) t = 60 ns, and gate shape time distribution

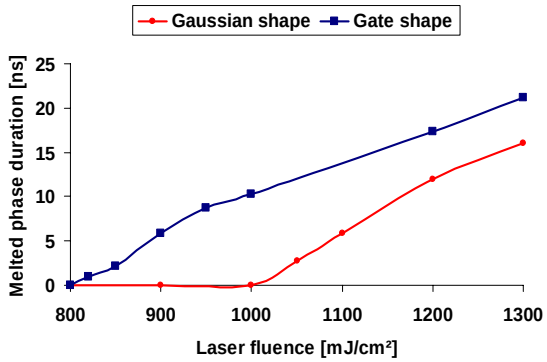

Figure 8: Melted phase duration versus laser fluence (F = 800 to 1300 mJ/cm²)

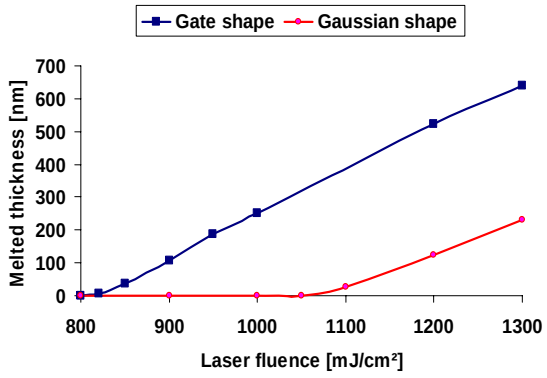

Figure 9: Melted thickness versus laser fluence (F = 800 to 1300 mJ/cm²)

5. Conclusion

Results on crystalline Si exhibit different values of the melting pool and the melting duration under the pulsed laser treatment. Typical values of working laser fluences (i.e. 800 to 1300 mJ/cm²) give a melting pool close to 500 nm that is namely higher than the amorphous Si layer (20 nm. For a gaussian shape time distribution (figure 9), the control of the melting kinetics is easier than in the gate shape one. However, in the first case, the melting threshold requires more energy.

The returned results show that investigation of melting kinetics should considered mainly in the range 800 to 1100 mJ/cm² (Figure 9), in order to refine the laser threshold.

Effort of computing will be focalized on the congruence of the numerical resolution between the space and the time steps to better control very fine melted structures as expected from our first objective.

7. Nomenclature and physical data

Table 1: Constants and global expressions used in COMSOL Multiphysics simulation

Name	Expression	Description
E	3.2e-8[J]	Absorbed Energy
tau	27e-9[s]	Laser pulse
S	4e-12[m^2]	Surface area
hc	10[W*m^-2*K^-1]	Heat coefficient transfert
Ttrans	1690[K]	Melting temperature
da	(6e-9)[m]	Absorption length
M	27.976926533e-3[kg/mol]	Molar mass
lm	1650[J/g]	Latent heat of fusion
rhoS	2320[kg/m^3]	Density of solid silicon
rhoL	2500[kg/m^3]	Density of liquid silicon
kthS	148[W/(m*K)]	Thermal conductivity of solid silicon
kthL	200[W/(m*K)]	Thermal conductivity of liquid silicon
CpS	710[J/(kg*K)]	Specific heat capacity of solid silicon
CpL	680[J/(kg*K)]	Specific heat capacity of liquid silicon
To	293[K]	Ambient temperature
R	0.59*(T<Ttrans)+0.65*(T>=Ttrans)	Silicon reflectivity
Pin	E/(S*tau)*((t<=27e-9)*(t>=0))[W/m²]	Gate input power
Pin2	E/(S*tau)*exp(-4*(t-tau)*(t-tau)/(tau*tau))[W/m²]	Gaussian input power
Gt1	(Pin*(1-R)/(da)*exp(y/da))[W/m^3]	First term of heat source
Gt2	(lm*rhoL/tau)*(T>=Ttrans)[W/m^3]	Second term of heat source
Gt	((Gt1-Gt2)*(Gt1>=Gt2))*(y<=0)[W/m^3]	Heat source
kth	kthS*(T<Ttrans)+kthL*(T>=Ttrans)[W/(m*K)]	Thermal conductivity
rho	rhoS*(T<Ttrans)+rhoL*(T>=Ttrans)[kg/m^3]	Density
Cp	CpS*(T<Ttrans)+CpL*(T>=Ttrans)[J/(kg*K)]	Specific heat capacity

6. References

1. J.S. Im, R.S. Sposili, M.A. Crowder: Appl. Phys. Lett. 70, 3434 (1997)

2. D Bauerle. Laser processing and Chemistry, second edition, Springer, p. 581.

3. C.P. Grigoropoulos, S. Moon, M. Lee, M. Hatano, K. Suzuki, Appl. Phys A 69 S295-S298 (1999)

4. Jiri Martan, Ph. D. THESIS, Universite of Orleans.. (2005).

5. G. Groos, M. Stutzmann: J. Non-Cryst. Solids 227, 938 (1998)

6. V.V. Gupta, H.J. Song, J.S. Im: Appl. Phys. Lett. 71, 99 (1997)

7. J. Tesar, N. Semmar, Thermal Effusivity of Metallic Thin Films: Comparison between 1D Multilayer analytical model and 2D Numerical Model Using COMSOL Multiphysics.

8. S.R Stiffler, M.O Thompson: Phys. Rev. Lett. 60, 2519 (1988)

9. Bianco N., Manca O., Nardini S., Tamburrino S., (2006)